Regioselectivity in 2-Methylbutane Hydroxylation Mediated by FeO^+ and FeO^{2+}

Takashi Yumura and Kazunari Yoshizawa*

Department of Molecular Engineering, Kyoto University, Sakyo-ku, Kyoto 606-8501, Japan

Received September 20, 2000

The regioselectivity in FeO^+- and FeO^{2+}-mediated hydroxylation reactions of 2-methylbutane that involves primary (1°), secondary (2°), and tertiary (3°) carbon atoms is discussed from theoretical calculations at the B3LYP DFT level. The energetics for four kinds of hydroxylation reactions of 2-methylbutane that lead to primary, secondary, and tertiary alcohols in a two-step concerted mechanism and in a radical mechanism are calculated and analyzed. With respect to H atom abstraction, a concerted mechanism via the four-centered transition state $\overline{\text{C}\cdots\text{H}\cdots\text{O}-\text{Fe}}$ is energetically more favorable than a radical mechanism via the linear transition state C···H····O−Fe in most cases, except for a case generating a tertiary carbon radical intermediate. The regioselectivity in the concerted mechanism prefers a secondary C−H bond dissociation and declines in the order 2° > 1° > 3°, whereas the regioselectivity in the radical mechanism prefers a tertiary C−H bond dissociation and declines in the order 3° > 2° > 1°. The kinetic isotope effects (KIEs) for the H atom abstraction from 2-methylbutane are analyzed on the basis of the transition state theory. Computed k_H/k_D values in the concerted mechanism do not show site dependence, while those in the radical mechanism have significant site dependence, the order of k_H/k_D values being 1° > 2° > 3°.

Introduction

Selective activation of small alkanes, especially of methane, is an important issue in modern catalytic chemistry.[1−9] A key step in the conversion of methane to methanol is in the C−H bond dissociation, because of the significant bond dissociation energy of the C−H bond (104 kcal/mol). Direct conversion of methane to methanol, which occurs in enzymatic[10,11] and gas-phase reactions,[12−14] is thermodynamically efficient compared to the commercial two-step process via synthesis gas ($CO + H_2O$).[5,6] Development of a direct process is thus required for efficient production of methanol. Schwarz and Schröder have studied in detail the conversion of methane to methanol by FeO^+,[12−14] which is formed from the reaction of Fe^+ with pulsed-in N_2O,[15] under cyclotron resonance conditions in the gas phase.[12] The bare FeO^+ complex is also able to activate various C−H and C−C bonds of alkanes, alkenes, and arenes.[12] We have analyzed from density functional theory (DFT) calculations an energetically preferred reaction pathway for the direct methane−methanol conversion by FeO^+.[16] This reaction occurs in a two-step manner, as shown in eq 1; it proceeds at the iron active center through concerted hydrogen and methyl migrations via the two transition states TS1 and TS2, respectively.

$$FeO^+ + CH_4 \rightarrow OFe^+(CH_4) \rightarrow [TS1] \rightarrow HO-Fe^+-CH_3 \rightarrow [TS2] \rightarrow Fe^+(CH_3OH) \rightarrow Fe^+ + CH_3OH \quad (1)$$

Hydrocarbon hydroxylations are efficiently catalyzed under physiological conditions by cytochrome P450[10]

* To whom correspondence should be addressed. Present address: Institute for Fundamental Research of Organic Chemistry, Kyushu University, Higashi-ku, Fukuoka 812-8581, Japan.

(1) (a) Shilov, A. E. *The Activation of Saturated Hydrocarbons by Transition Metal Complexes*; Reidel: Dordrecht, The Netherlands, 1984. (b) Shilov, A. E. *Metal Complexes in Biomimetic Chemical Reactions*; CRC: Boca Raton, FL, 1996.

(2) (a) Bergman, R. G. *Science* **1984**, *223*, 902. (b) Arndtsen, B. A.; Bergman, R. G.; Mobley, T. A.; Peterson, T. H. *Acc. Chem. Res.* **1995**, *28*, 154.

(3) Hill, C. L., Ed. *Activation and Functionalization of Alkanes*; Wiley: New York, 1989.

(4) Davies, J. A.; Watson, P. L.; Liebman, J. F.; Greenberg, A. *Selective Hydrocarbon Activation*; VCH: New York, 1990.

(5) (a) Crabtree, R. H. *Chem. Rev.* **1985**, *85*, 245. (b) Crabtree, R. H. *Chem. Rev.* **1995**, *95*, 987.

(6) Gesser, H. D.; Hunter, N. R.; Prakash, C. B. *Chem. Rev.* **1985**, *85*, 237.

(7) Lunsford, J. H. *Angew. Chem., Int. Ed. Engl.* **1995**, *34*, 970.

(8) Schneider, J. J. *Angew. Chem., Int. Ed. Engl.* **1996**, *35*, 1068.

(9) Hall, C.; Perutz, R. N. *Chem. Rev.* **1996**, *96*, 3125.

(10) (a) *Cytochrome P450: Structure, Mechanism, and Biochemistry*, 2nd ed.; Ortiz de Montellano, P. R., Ed.; Plenum: New York, 1995. (b) Sono, M.; Roach, M. P.; Coulter, E. D.; Dawson, J. H. *Chem. Rev.* **1996**, *96*, 2841.

(11) (a) Wallar, B. J.; Lipscomb, J. D. *Chem. Rev.* **1996**, *96*, 2625. (b) Que, L., Jr.; Dong, Y. *Acc. Chem. Res.* **1996**, *29*, 190. (c) Feig, A. L.; Lippard, S. J. *Chem. Rev.* **1994**, *94*, 759. (d) Lipscomb, J. D. *Annu. Rev. Microbiol.* **1994**, *48*, 371.

(12) Schröder, D.; Schwarz, H. *Angew. Chem., Int. Ed. Engl.* **1995**, *34*, 1973.

(13) (a) Schröder, D.; Schwarz, H. *Angew. Chem., Int. Ed. Engl.* **1990**, *29*, 1433. (b) Schröder, D.; Fiedler, A.; Hrusák, J.; Schwarz, H. *J. Am. Chem. Soc.* **1992**, *114*, 1215. (c) Schröder, D.; Schwarz, H.; Clemmer, D. E.; Chen, Y.-M.; Armentrout, P. B.; Baranov, V. I.; Böhme, D. K. *Int. J. Mass Spectrom. Ion Processes* **1997**, *161*, 175.

(14) (a) Schröder, D.; Schwarz, H. *Helv. Chim. Acta* **1992**, *75*, 1281. (b) Becker, H.; Schröder, D.; Zummack, W.; Schwarz, H. *J. Am. Chem. Soc.* **1994**, *116*, 1096. (c) Ryan, M. F.; Stöckigt, D.; Schwarz, H. *J. Am. Chem. Soc.* **1994**, *116*, 9565.

(15) (a) Kappes, M. M.; Staley, R. H. *J. Am. Chem. Soc.* **1981**, *103*, 1286. (b) Kappes, M. M.; Staley, R. H. *J. Phys. Chem.* **1981**, *85*, 942.

(16) (a) Yoshizawa, K.; Shiota, Y.; Yamabe, T. *Chem. Eur. J.* **1997**, *3*, 1160. (b) Yoshizawa, K.; Shiota, Y.; Yamabe, T. *J. Am. Chem. Soc.* **1998**, *120*, 564. (c) Yoshizawa, K.; Shiota, Y.; Yamabe, T. *Organometallics* **1998**, *17*, 2825.

10.1021/om000811b CCC: $20.00
Publication on Web 03/02/2001

and methane monooxygenase (MMO).[11] Lippard, Newcomb, and collaborators reported regioselective variations of H atom abstraction from methylcubane with *tert*-butoxyl radical, cytochrome P450, and sMMO from *Methylococcus capsulatus* (Bath),[17] demonstrating that cytochrome P450 hydroxylated all positions of methylcubane, whereas the sMMO system hydroxylated only the methyl position. These biochemical regioselective variations are in remarkable contrast to a strong preference for the cubyl hydrogen abstraction by *tert*-butoxyl radical. Jin and Lipscomb subsequently reported that sMMO from *Methylosinus trichosporium* (OB3b) hydroxylated all positions of methylcubane and that a major product was derived from rearrangement of cubylcarbinyl radical.[18] On the other hand, Lippard et al.[19] recently suggested that both sMMO systems oxidized methylcubane into 1-homocubanol derived from a cationic species as a major product. Thus, the regioselectivity of H atom abstraction from alkanes is an important index in considering the mechanism of hydroxylation reactions.

C−H bond dissociation energies of higher alkanes range from 98 kcal/mol for a primary position to 93 kcal/mol for a tertiary position,[20] and it is therefore interesting to see how the C−H bonds of primary (1°), secondary (2°), and tertiary (3°) positions are activated. According to a textbook,[21] the relative reactivity of alkanes in biological hydroxylations generally declines in the order 2° > 3° > 1°. This is different from a general trend expected from a radical mechanism (3° > 2° > 1°). Schwarz et al. have examined C−H bond activation reactions of norbornane by FeO^+ from ion cyclotron resonance experiments and DFT calculations.[22] Their DFT calculations show that a two-state reactivity mechanism[23] plays a dominant role in the activation of both *exo* and *endo* C−H bonds.[22b] Koch et al. have investigated Fe^+- and Co^+-mediated C−H bond activation of ethane and Fe^+-mediated C−H bond activation of propane,[24] and Siegbahn et al. have investigated Y-, Zr-, Nb-, Rh-, and Pd-mediated C−H bond activation of ethane and cyclopropane and Ni^+-mediated C−H bond activation of propane.[25] In particular, the regioselectivity in the activation of propane[24c,25c] is an intriguing subject in that propane involves primary and secondary carbon atoms in it.

Scheme 1

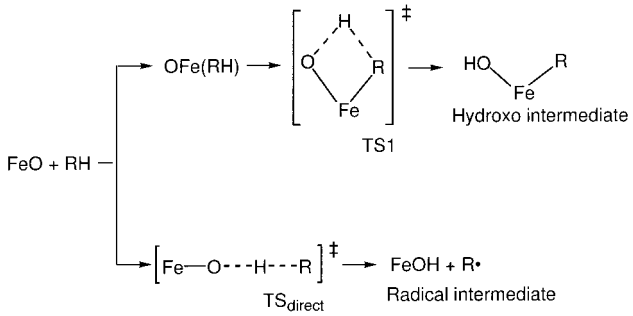

2-Methylbutane (C_5H_{12}) is an interesting substrate in that it is the smallest alkane involving primary, secondary, and tertiary carbon atoms. It is useful to see how this alkane is oxidized into primary, secondary, and tertiary alcohols. The subject of this paper is to analyze the regioselectivity of hydroxylation reactions of 2-methylbutane by FeO^+ and FeO^{2+} on the basis of the concerted mechanism via the four-centered transition state (TS1) and the radical mechanism via the transition state with a linear C−H−O array (TS_{direct}) (see Scheme 1). The most striking difference between the two mechanisms is in whether the iron active center is directly concerned or not. We discuss the reaction pathways and their energetics for possible oxidation reactions of 2-methylbutane into four kinds of alcohols.

Method of Calculation

We carried out quantum-chemical calculations on the basis of the hybrid Hartree−Fock/density functional theory (B3LYP) method[26,27] using the Gaussian 94 ab initio program package.[28] The B3LYP method consists of Slater exchange, Hartree−Fock exchange, the exchange functional of Becke,[26] the correlation functional of Lee, Yang, and Parr (LYP),[27] and the correlation functional of Vosko, Wilk, and Nusair (VWN).[29] We optimized local energy minima corresponding to the reactants, products, and intermediates and saddle points corresponding to the transition states. Harmonic vibrational frequencies were systematically computed to confirm that each optimized geometry corresponds to a local minimum that has only real frequencies or a saddle point that has only one imaginary frequency. For the Fe atom we used the (14s9p5d) primitive set of Wachters supplemented with polarization f functions ($\alpha = 1.05$), resulting in a (611111111|51111|311|1) [9s5p3d1f] contraction,[30] and for the H, C, and O atoms we used the D95** basis set, a standard double-ζ basis set with polarization function.[31] The spin-unrestricted method was applied to the open-shell systems. It was confirmed from computed $\langle S^2 \rangle$

(17) Choi, S.-Y.; Eaton, P. E.; Hollenberg, P. F.; Liu, K. E.; Lippard, S. J.; Newcomb, M. Putt, D. A.; Upadhyaya, S. P.; Xiong, Y. *J. Am. Chem. Soc.* **1996**, *118*, 6547.
(18) Jin, Y.; Lipscomb, J. D. *Biochemistry* **1999**, *38*, 6178.
(19) Choi, S.-Y.; Eaton, P. E.; Kopp, D. A.; Lippard, S. J.; Newcomb, M.; Shen, R. *J. Am. Chem. Soc.* **1999**, *121*, 12198.
(20) (a) McMillen, D. F.; Golden, D. M. *Annu. Rev. Phys. Chem.* **1982**, *33*, 493. (b) Solomons, T. W. G. *Organic Chemistry*, 5th ed.; Wiley: New York, 1996.
(21) Faber, K. *Biotransformations in Organic Chemistry*, 3rd ed.; Springer-Verlag: Berlin, 1997.
(22) (a) Schwarz, J.; Schwarz, H. *Helv. Chim. Acta* **1995**, *78*, 1013. (b) Harris, N.; Shaik, S.; Schröder, D.; Schwarz, H. *Helv. Chim. Acta* **1999**, *82*, 1784.
(23) (a) Shaik, S.; Danovich, D.; Fiedler, A.; Schröder, D.; Schwarz, H. *Helv. Chim. Acta* **1995**, *78*, 1393. (b) Schröder, D.; Shaik, S.; Schwarz, H. *Acc. Chem. Res.* **2000**, *33*, 139.
(24) (a) Holthausen, M. C.; Fiedler, A.; Schwarz, H.; Koch, W. *J. Phys. Chem.* **1996**, *100*, 6236. (b) Holthausen, M. C.; Koch, W. *J. Am. Chem. Soc.* **1996**, *118*, 9932. (c) Holthausen, M. C.; Koch, W. *Helv. Chim. Acta* **1996**, *79*, 1939.
(25) (a) Carroll, J. J.; Haug, K. L.; Weisshaar, J. C.; Blomberg, M. R. A.; Siegbahn, P. E. M.; Svensson, M. *J. Phys. Chem.* **1995**, *99*, 13955. (b) Carroll, J. J.; Weisshaar, J. C.; Siegbahn, P. E. M.; Wittborn, C. A. M.; Blomberg, M. R. A. *J. Phys. Chem.* **1995**, *99*, 14388. (c) Yi, S. S.; Blomberg, M. R. A.; Siegbahn, P. E. M.; Weisshaar, J. C. *J. Phys. Chem. A* **1998**, *102*, 395.
(26) (a) Becke, A. D. *Phys. Rev. A* **1988**, *38*, 3098. (b) Becke, A. D. *J. Chem. Phys.* **1993**, *98*, 5648. (c) Stephens, P. J.; Devlin, F. J.; Chabalowski, C. F.; Frisch, M. J. *J. Phys. Chem.* **1994**, *98*, 11623.
(27) Lee, C.; Yang, W.; Parr, R. G. *Phys. Rev. B* **1988**, *37*, 785.
(28) Frisch, M. J.; Trucks, G. W.; Schlegel, H. B.; Gill, P. M. W.; Johnson, B. G.; Robb, M. A.; Cheeseman, J. R.; Keith, T. A.; Petersson, G. A.; Montgomery, J. A.; Raghavachari, K.; Al-Laham, M. A.; Zakrzewski, V. G.; Ortiz, J. V.; Foresman, J. B.; Cioslowski, J.; Stefanov, B. B.; Nanayakkara, A.; Challacombe, M.; Peng, C. Y.; Ayala, P. Y.; Chen, W.; Wong, M. W.; Andres, J. L.; Replogle, E. S.; Gomperts, R.; Martin, R. L.; Fox, D. J.; Binkley, J. S.; Defrees, D. J.; Baker, J.; Stewart, J. J. P.; Head-Gordon, M.; Gonzalez, C.; Pople, J. A. *Gaussian 94*; Gaussian Inc.: Pittsburgh, PA, 1995.
(29) Vosko, S. H.; Wilk, L.; Nusair, M. *Can. J. Phys.* **1980**, *58*, 1200.
(30) Wachters, A. J. H. *J. Chem. Phys.* **1970**, *52*, 1033.
(31) Dunning, T. H.; Hay, P. J. In *Modern Theoretical Chemistry*; Schaefer, H. F., Ed.; Plenum: New York, 1976.

Scheme 2

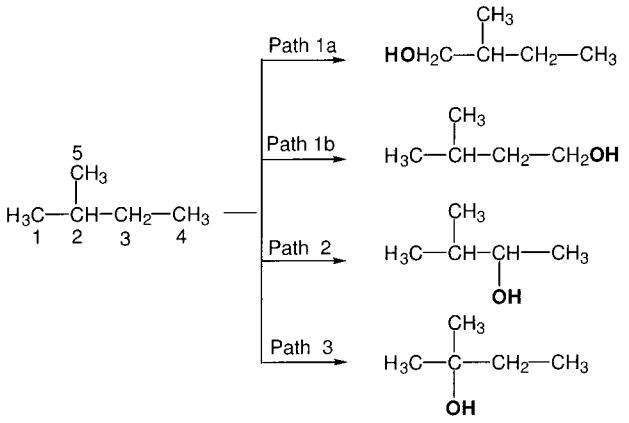

values that spin contamination included in the calculations is within 0.6% after annihilation of higher spin states. We computed the bond dissociation energy of the $^6\Sigma^+$ state of FeO^+ to look at the applicability of this DFT method. This quantity was computed to be 75.2 kcal/mol, which is in good agreement with an experimental value of 81.4 ± 1.4 kcal/mol.[32]

We calculated the KIEs for H(D) atom abstractions using the transition state theory, which leads to the expression[33]

$$\frac{k(\mathrm{H})}{k(\mathrm{D})} = \left(\frac{[m\ (\mathrm{D})][m(\mathrm{H})^{\#}]}{[m(\mathrm{H})][m(\mathrm{D})^{\#}]}\right)^{3/2} \times \left(\frac{[I_x(\mathrm{D})][I_y(\mathrm{D})][I_z(\mathrm{D})]}{[I_x(\mathrm{H})][I_y(\mathrm{H})][I_z(\mathrm{H})]}\right)^{1/2} \times \left(\frac{[I_x(\mathrm{H})^{\#}][I_y(\mathrm{H})^{\#}][I_z(\mathrm{H})^{\#}]}{[I_x(\mathrm{D})^{\#}][I_y(\mathrm{D})^{\#}][I_z(\mathrm{D})^{\#}]}\right)^{1/2} \times \frac{q_v(\mathrm{D})}{q_v(\mathrm{H})}\frac{q_v(\mathrm{H})^{\#}}{q_v(\mathrm{D})^{\#}} \exp\left(-\frac{E(\mathrm{H})^{\#} - E(\mathrm{D})^{\#}}{RT}\right) \quad (2)$$

where H and D stand for the hydrogen and deuterium-substituted forms, respectively, q_v stands for the vibrational partition function, I values are principal moments of inertia, m is the molecular mass, and $E^{\#}$ is the activation energy measured from the reactant complex on each potential energy surface (it includes zero point vibrational energies (ZPVEs).

Results and Discussion

C−H Bond Strengths of 2-Methylbutane. In this paper, we consider possible hydroxylation reactions of 2-methylbutane. This alkane has four kinds of H atoms and can thus generate four kinds of alcohols as products: 2-methyl-1-butanol (primary alcohol), 3-methyl-1-butanol (primary alcohol), 3-methyl-2-butanol (secondary alcohol), and 2-methyl-2-butanol (tertiary alcohol). In Scheme 2, we label the carbon atoms of 2-methylbutane and show the four reaction pathways. Path 1a is the reaction pathway leading to a primary alcohol, path 1b is that leading to another primary alcohol, path 2 is that leading to the secondary alcohol, and path 3 is that leading to the tertiary alcohol. The regioselectivity should be determined by the energetics of the H atom abstractions that occur in the initial stages of these hydroxylation reactions.

Chart 1

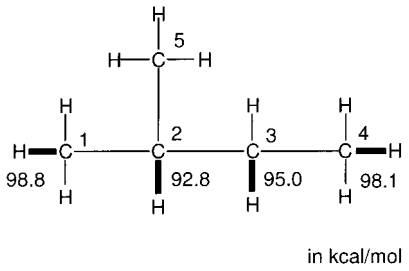

Before discussing the energetics of the hydroxylation reactions mediated by FeO^+ and FeO^{2+}, we describe the variation in C−H bond dissociation energies of 2-methylbutane. Chart 1 shows computed C−H bond dissociation energies on the C1, C2, C3, and C4 atoms of 2-methylbutane, which decline in the order

primary C1−H > primary C4−H > secondary C3−H > tertiary C2−H

The tertiary C2−H bond of 2-methylbutane is the weakest (92.8 kcal/mol), followed by the secondary C3−H bonds (95.0 kcal/mol), the primary C4−H bonds (98.1 kcal/mol), and the primary C1−H bonds (98.8 kcal/mol). This DFT result is fully consistent with an experimental result regarding ethane, propane, *tert*-butane, *sec*-butane, and cyclopentane: the tertiary C−H bond dissociation energy is ∼94 kcal/mol, the secondary C−H bond dissociation energy is ∼96 kcal/mol, and the primary C−H bond dissociation energy is ∼100 kcal/mol.[34] Thus, the method of choice is appropriate for our theoretical considerations.

2-Methylbutane Hydroxylations by FeO^+. Let us first look at the FeO^+-mediated oxidation reactions of 2-methylbutane to the product alcohols. It has been shown in previous studies[16] that in methane hydroxylation by FeO^+ the reacting system should pass over TS1 on the low-spin quartet-state potential energy surface. We can confine our discussions to the 2-methylbutane hydroxylations by FeO^+ ($^4\Delta$)[35] in the concerted mechanism, although two-state reactivity[23] is an essential feature in the C−H bond activation reactions, because there are many possible reaction species to be considered in the four reaction pathways.[36] On the other hand, both sextet and quartet states of FeO^+ are considered in the radical mechanism.

The hydroxylation reactions in the concerted mechanism are expected to occur as in eq 3. In the initial

$$FeO^+ + C_5H_{12} \rightarrow OFe^+(C_5H_{12}) \rightarrow [TS1] \rightarrow HO{-}Fe^+{-}C_5H_{11} \rightarrow [TS2] \rightarrow Fe^+(C_5H_{11}OH) \rightarrow Fe^+ + C_5H_{11}OH \quad (3)$$

stages of the reactions, the reactants come into contact to form the reactant complex $OFe^+(C_5H_{12})$. An H atom abstraction via the four-centered transition state TS1

(32) Loh, S. K.; Fisher, E. R.; Lian, L.; Schultz, R. H.; Armentrout, P. B. *J. Phys. Chem.* **1989**, *93*, 2601.
(33) (a) McQuarrie, D. A. *Statistical Thermodynamics*; University Science Books: Mill Valley, CA, 1973. (b) Filatov, M.; Shaik, S. *J. Phys. Chem. A* **1998**, *102*, 3835.
(34) Castelhano, A. L.; Griller, D. *J. Am. Chem. Soc.* **1982**, *104*, 3655.
(35) According to ref 23a, the $^4\Phi$ state lies 0.2 eV below the $^4\Delta$ state from CASPT2D calculations. However, this discrepancy is not so important in discussing the energy profile of the quartet reaction pathway because the relevant reaction species have no symmetry.

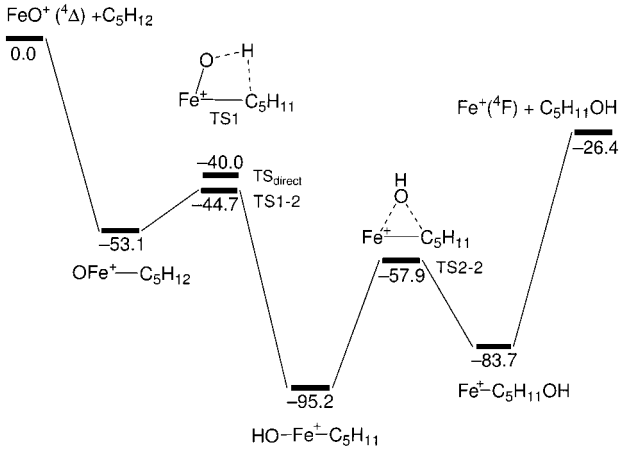

Figure 1. Potential energy diagram for the conversion of 2-methylbutane into 3-methyl-2-butanol by FeO^+ (path 2) in the quartet state at the B3LYP/(Wachters + D95**) level of theory. Note that the reaction proceeds in a two-step manner, via TS1-2 and TS2-2. Relative energies, which include zero-point vibrational energy corrections, are given in kcal/mol.

leads to an iron−hydroxo intermediate that involves OH and C_5H_{11} groups as ligands. An important occurrence in TS1 is the formation of an O−H bond as well as the cleavage of a C−H bond. There are four kinds of iron−hydroxo intermediates that depend on which hydrogen atom is abstracted (see Scheme 2). An iron−hydroxo intermediate is transformed via the three-centered transition state TS2 into the final complex $Fe^+(C_5H_{11}OH)$, and each reaction is completed after releasing a product alcohol. TS2 can be viewed as a transition state for the rebound step.

There are three reaction intermediates and two transition states along each concerted reaction pathway, except for the reactants and the products. We optimized all the reaction species for the four kinds of reaction pathways indicated in Scheme 2. Computed energies of the reactant species measured from the dissociation limit (FeO^+ ($^4\Delta$) + C_5H_{12}) are listed in Table 1. Let us look in detail at the conversion of 2-methylbutane to the secondary alcohol along path 2, which is energetically the most favorable reaction pathway among those possible. After discussing the energetics of path 2, we will refer to those of the other reaction pathways. Figure 1 shows a computed energy diagram for the conversion of 2-methylbutane to the secondary alcohol in the quartet state, and Figure 2 presents optimized geometries for the reaction species relevant to this hydroxylation. The reactant complex exhibits an η^2-C_5H_{12} mode in which the Fe ion is close to two carbon atoms of the substrate; the Fe−C1 and the Fe−C3 bonds were computed to be 2.339 and 2.137 Å in length, respectively. These Fe−C bonds are longer than the regular Fe−C bonds (∼1.9 Å) of the hydroxo intermediate, as seen in Figure 2.

In the reactant complex, the total charge of 2-methylbutane was calculated to be +0.24 at the B3LYP level.

Table 1. Computed Energies (in kcal/mol) of the Reaction Species Measured from the Dissociation Limit (FeO^+ ($^4\Delta$) + C_5H_{12}) along the Four Kinds of Reaction Pathways for 2-Methylbutane Hydroxylation Reactions by FeO^+

	path 1a	path 1b	path 2	path 3
reactant complex (^{4}A)	−54.6		−53.1	
TS1 (^{4}A)	−40.4	−43.2	−44.7	−40.2
hydroxy intermediate (^{4}A)	−93.3	−91.7	−95.2	−93.0
TS2 (^{4}A)	−63.5	−54.5	−57.9	−53.5
product complex (^{4}A)	−81.4	−82.5	−83.7	−86.8
product (^{1}A) + Fe^+ (^{4}F)	−23.1	−22.6	−26.4	−28.6
TS_{direct} (^{4}A)	−41.6	−42.3	−40.0	−41.2

Once this complex is formed, the C−H bonds are highly activated, due to the depopulation of the C−H bonding orbitals. After the reactant complex is formed, one of the H atoms is abstracted via TS1-2. The transition vector of TS1-2 represents an H atom migration from the secondary C3 atom to the O atom of FeO^+. Thus, this structure should correctly connect the reactant complex and the iron−hydroxo intermediate. Since the activation energy for the C3−H bond dissociation via TS1-2 was computed to be −44.7 kcal/mol relative to the dissociation limit, this reaction is expected to easily take place.

We next turn to the iron−hydroxo intermediate in path 2 that leads to the secondary alcohol via TS2-2. This intermediate is the most stable reaction species in the reaction pathway, and therefore it would act as the central species for the hydroxylation of 2-methylbutane. In the three-centered transition state TS2-2, the Fe−C bond is cleaved and instead the C−O bond is newly formed. The transition vector of TS2-2 represents an O atom migration to the secondary C3 atom of the 2-methylbutane fragment. The barrier height of TS2-2 was computed to be 37.3 kcal/mol relative to the hydroxo intermediate and −57.9 kcal/mol relative to the dissociation limit, and in view of its energy profile this electronic process is considered to easily take place.

Finally, we turn our attention to the product complex in Figure 2. This is a complex of 3-methyl-2-butanol and Fe^+. The Fe−O bond length was computed to be 1.958 Å, which is clearly larger than those of the reactant complex and of the hydroxo intermediate. It is a typical coordinate bond. We therefore expect that the Fe−O bond in the product complex should be cleaved, resulting in the release of the product 3-methyl-2-butanol. Actually, the binding energy between 3-methyl-2-butanol and Fe^+ was calculated to be 57.3 kcal/mol relative to the product complex and −26.4 kcal/mol relative to the dissociation limit.

Having described the concerted mechanism, let us next consider the radical mechanism, in which an H atom is directly abstracted by the O atom of the FeO^+ complex. The relevant transition state with a nearly linear C−H−O array is termed TS_{direct} throughout this paper. This abstraction reaction gives rise to an iron−hydroxo species and an alkyl radical intermediate, followed by recombination of these reaction species and the release of a product alcohol. The transition vector of TS_{direct}-2 indicates a dissociation into the FeOH and C_5H_{11} fragments, as shown in Figure 3. The C3−H bond length of TS_{direct}-2 was computed to be 1.209 Å, the O−H bond length 1.304 Å, and the C−H−O angle 171.4°. It is interesting to compare the energetics of the concerted

(36) We carried out B3LYP calculations of the energies required for C−H bond dissociation via four-centered transition states TS1 mediated by FeO^+ ($^6\Sigma^+$) in paths 2 and 3, as indicated in Scheme 2. However, we could not obtain TS1's mediated by FeO^+ ($^6\Sigma^+$) in paths 1a and 1b. The computed C−H bond activation energies via TS1 mediated by FeO^+ ($^6\Sigma^+$) are 10.2 and 9.0 kcal/mol higher than those via TS1 mediated by FeO^+ ($^4\Delta$) in paths 2 and 3, respectively.

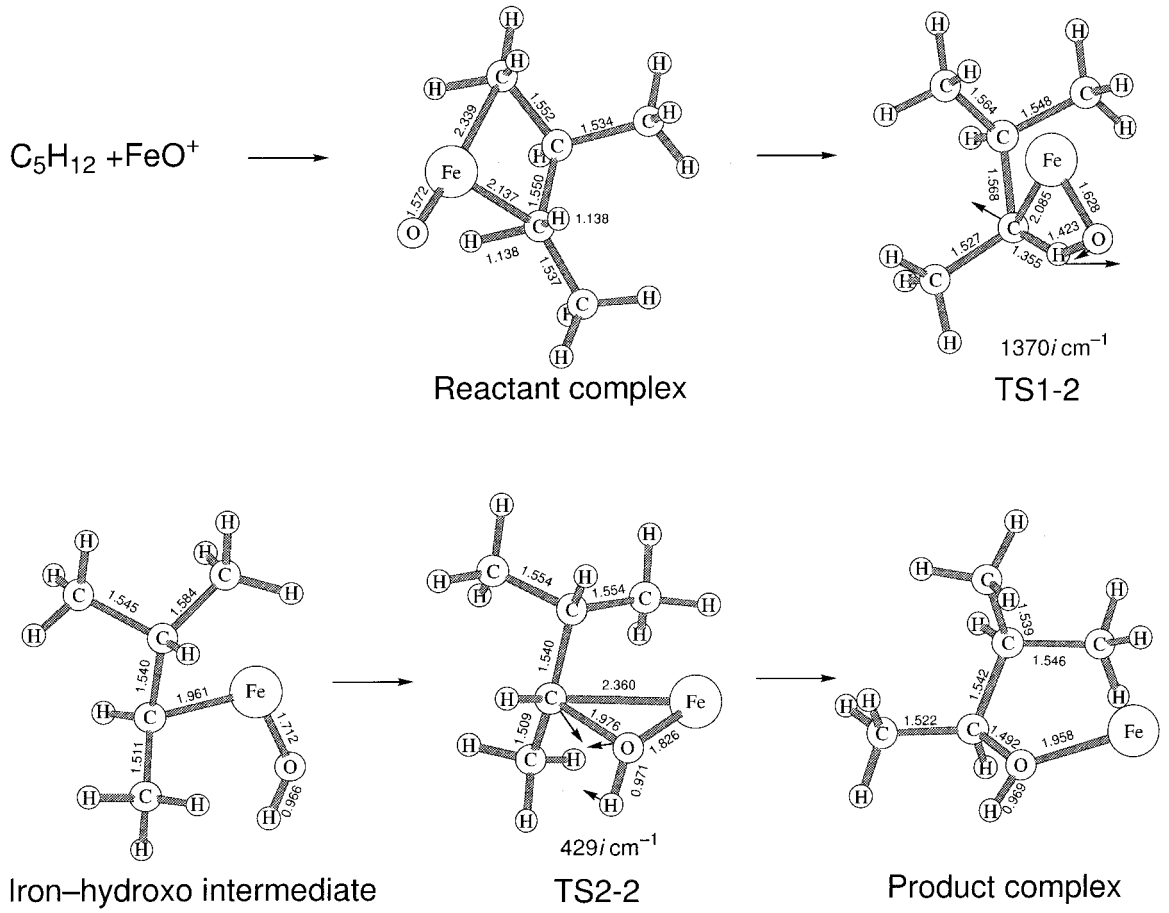

Figure 2. Ball-and-stick structures of the reaction intermediates and the transition states for the conversion of 2-methylbutane into 3-methyl-2-butanol by FeO^+ (path 2) in the quartet state. Bond lengths are in Å.

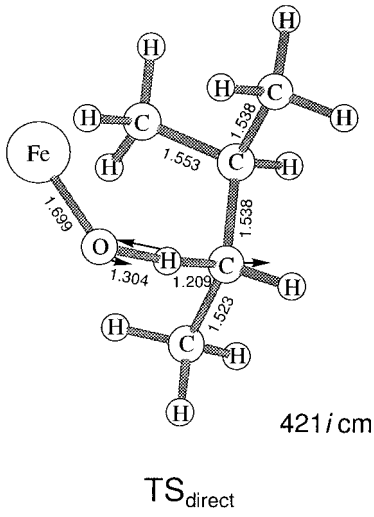

Figure 3. Ball-and-stick structures of TS_{direct} for the conversion of 2-methylbutane into 3-methyl-2-butanol by FeO^+ in the quartet state. Bond lengths are in Å.

mechanism and the radical mechanism. In path 2, TS_{direct}-2 was computed to lie 4.7 kcal/mol above TS1-2. Thus, the concerted reaction pathway is energetically more favorable than the radical reaction pathway in the FeO^+-mediated 2-methylbutane hydroxylation along path 2.

Finally, we look at the energetics for the other 2-methylbutane hydroxylations along paths 1a, 1b, and 3. In path 1a, an H atom attached to the primary C1 atom is abstracted by FeO^+ to result in 2-methyl-1-butanol. The overall reaction in path 1a is exothermic by 23.1 kcal/mol. The activation energy for the C1−H bond dissociation via TS1-1a was computed to be −40.4 kcal/mol relative to the dissociation limit. The hydroxo intermediate that lies 93.3 kcal/mol below the dissociation limit is transformed into a final complex via TS2-1a. In path 1b, a C4−H bond of 2-methylbutane is cleaved by FeO^+ to finally lead to 3-methyl-1-butanol. The activation energy for the C4−H bond dissociation via TS1-1b was computed to be −43.2 kcal/mol relative to the dissociation limit. The resultant iron−hydroxo intermediate is converted into 3-methyl-1-butanol via an O atom migration to the primary C4 atom of the 2-methylbutane fragment. The overall reaction in path 1b is 22.6 kcal/mol exothermic. In the initial stages of path 3, the H atom attached to the tertiary C2 atom is

Table 2. Computed Energies of the Reaction Species Measured from the Dissociation Limit (FeO^{2+} ($^5\Sigma$) + C_5H_{12}) along the Four Kinds of Reaction Pathways for 2-Methylbutane Hydroxylation Reactions by FeO^{2+}

	path 1a	path 1b	path 2	path 3
reactant complex (^{5}A)	−140.1		−136.7	
TS1 (^{5}A)	−126.5	−132.0	−133.6	−129.6
hydroxy intermediate (^{5}A)	−193.5	−191.9	−205.8	−211.5
TS2 (^{5}A)	−187.0	−182.4	−195.2	−200.6
product complex (^{5}A)	−223.3	−224.5	−225.3	−224.6
product (^{1}A) + Fe^{2+} (^{5}D)	−63.2	−62.7	−66.5	−68.8
TS_{direct} (^{5}A)	−124.5	−124.3	−129.2	−140.1

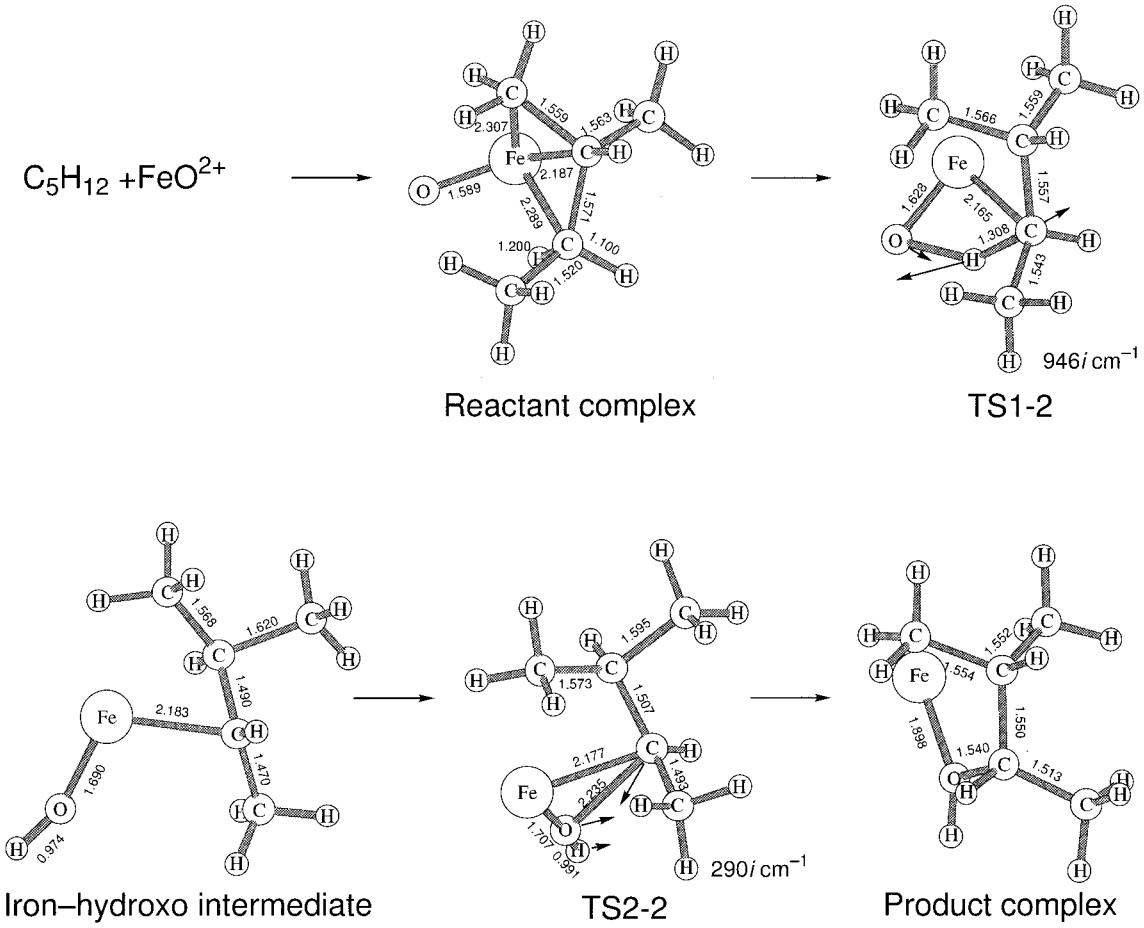

Figure 4. Ball-and-stick structures of the reaction intermediates and the transition states for the conversion of 2-methylbutane into 3-methyl-2-butanol by FeO^{2+} (path 2) in the quintet state. Bond lengths are in Å.

abstracted by FeO^+. Since a strong preference of the tertiary C2−H bond dissociation is expected in the radical mechanism, it is interesting to investigate whether the tertiary C2−H bond dissociation can easily occur or not in the concerted mechanism. The activation energy for the C2−H bond dissociation via TS1-3 was computed to be −40.2 kcal/mol relative to the dissociation limit. However, the radical mechanism is energetically more favorable than the concerted mechanism in path 3. In contrast to the other reaction pathways, our DFT computations predicted that the tertiary C−H bond should be cleaved in the radical mechanism rather than in the concerted mechanism; the transition state of the direct tertiary C2−H bond dissociation TS_{direct}-3 lies 1.0 kcal/mol below the corresponding TS1-3. However, it may be more appropriate to say that these two mechanisms are energetically comparable in path 3, since the energy difference is small.

2-Methylbutane Hydroxylations by FeO^{2+}. Since two-state reactivity is unlikely to play an essential role in the reactivity of the isoelectronic MnO^+ and FeO^{2+} systems, as confirmed from DFT calculations,[16b,c] here we considered the $^5\Sigma^+$ state of FeO^{2+} in our analyses. Computed energies of the reaction species of the hydroxylation reactions of 2-methylbutane by FeO^{2+} are listed in Table 2. First, we discuss the conversion of 2-methylbutane to the secondary alcohol along path 2. Figure 4 presents optimized geometries for the reaction intermediates and the transition states along this reaction pathway. Most of the geometries optimized for the reaction species in the FeO^{2+} case are essentially identical with those in the FeO^+ case, except for the reactant complex. The reactant complex involving 2-methylbutane exhibits an η^3-C_5H_{12} mode in which the Fe ion is close to three carbon atoms of the substrate. The distances of the Fe−C bonds were computed to be 2.187, 2.289, and 2.307 Å, which are smaller than those of the reactant complex in the FeO^+ case. Significant electron transfer occurs from 2-methylbutane to FeO^{2+}; the total charge of 2-methylbutane was computed to be +0.80, which is larger than +0.24 in the FeO^+ case.

Figure 5 shows a computed energy diagram along path 2 for the FeO^{2+}-mediated conversion of 2-methylbutane into the secondary alcohol. The overall reaction is 66.5 kcal/mol exothermic on the quintet potential energy surface. The energetics of the hydroxylation reaction by FeO^{2+} is a little different from that of the same hydroxylation reaction by FeO^+. The binding energy between 2-methylbutane and FeO^{2+} was computed to be 136.7 kcal/mol. The activation energy of the secondary C3−H bond cleavage was computed to be −133.6 kcal/mol relative to the dissociation limit. The magnitude of the electron transfer from the filled C−H bonding orbitals in the $FeO^{2+}(C_5H_{12})$ complex is larger than that in the $FeO^+(C_5H_{12})$ complex, and therefore a C3−H bond is cleaved by FeO^{2+} more efficiently than by FeO^+. Figure 5 shows that TS1-2 lies 4.4 kcal/mol below TS_{direct}-2; thus, the concerted mechanism via

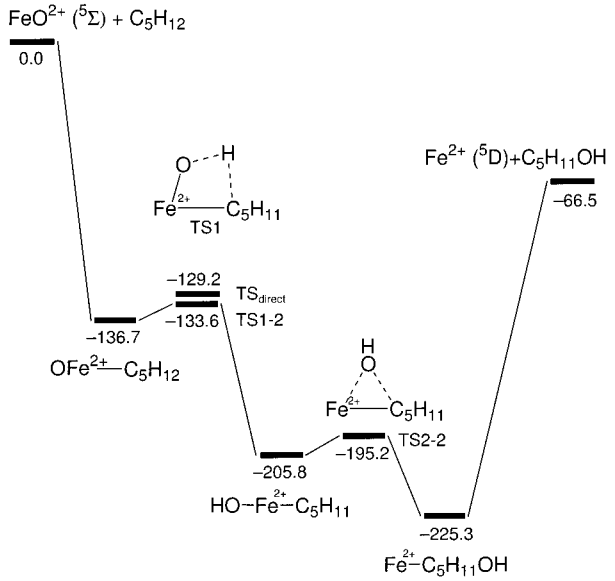

Figure 5. Potential energy diagram for the conversion of 2-methylbutane into 3-methyl-2-butanol by FeO^{2+} (path 2) in the quintet state at the B3LYP/(Wachters + D95**) level of theory. Note that the reaction proceeds in a two-step manner, via TS1-2 and TS2-2. Relative energies, which include zero-point vibrational energy corrections, are in kcal/mol.

TS1-2 is energetically more favorable than the radical mechanism via TS_{direct}-2 in path 2. The hydroxo intermediate lies 205.8 kcal/mol below the dissociation limit. The barrier height of TS2-2 relative to the hydroxo intermediate was computed to be 10.6 kcal/mol.

Next, we consider a potential-energy diagram for 2-methylbutane hydroxylation along the other reaction pathways. In path 1a, an H atom attached to the primary C1 atom is abstracted by FeO^{2+} to result in 2-methyl-1-butanol. The overall reaction is 63.2 kcal/mol exothermic. The activation energy for the C1−H bond dissociation via TS1-1a was computed to be −126.5 kcal/mol relative to the dissociation limit. An H atom abstraction after the formation of a reactant complex leads to an iron−hydroxo intermediate, which lies −193.5 kcal/mol below the dissociation limit and is subsequently transformed into a product complex via the three-centered transition state TS2-1a. TS_{direct}-1a lies 2.0 kcal/mol above TS1-1a in this reaction pathway. In path 1b, an H atom attached to the primary C4 atom is abstracted by FeO^{2+}. The overall reaction is 62.7 kcal/mol exothermic. The C4−H bond dissociation energy via TS1-1b was computed to be −132.0 kcal/mol relative to the dissociation limit. After the C4−H bond is abstracted by FeO^{2+}, an iron-hydroxo intermediate is formed. This intermediate is converted into 3-methyl-1-butanol via TS2-1b. TS_{direct}-1b lies 7.7 kcal/mol above TS1-1b in path 1b. Therefore, the concerted mechanism proceeds more easily than the radical mechanism in both reaction pathways that lead to the primary alcohols. In path 3, the H atom attached to the tertiary C2 atom is abstracted by FeO^{2+}. The activation energy for the C2−H bond dissociation via TS1-3 was computed to be −129.6 kcal/mol relative to the dissociation limit, TS1-3 lying 10.7 kcal/mol above TS_{direct}-3, in remarkable contrast to the other cases. Thus, the direct abstraction in the radical mechanism is energetically more favorable than the concerted process in the tertiary C−H bond dissociation.

Table 3. Computed C−H Bond Activation Energies of 2-Methylbutane by FeO^+ via the Concerted Mechanism or the Radical Mechanism Measured from the Dissociation Limit

	energy (au)	ZPVE (kcal/mol)	rel energy (kcal/mol)
C_5H_{12} (^{1}A)	−197.803 231 9	100.3	
FeO^+ ($^4\Delta$)	−1 338.517 005 7	1.0	
TS1-1a (^{4}A)	−1 536.381 742 6	99.5	−40.4
TS1-1b (^{4}A)	−1 536.386 410 1	99.6	−43.2
TS1-2 (^{4}A)	−1 536.387 924 1	99.1	−44.7
TS1−3 (^{4}A)	−1 536.381 293 5	99.4	−40.2
TS_{direct}-1a (^{4}A)	−1 536.381 781 8	98.3	−41.6
TS_{direct}-1b (^{4}A)	−1 536.382 592 2	98.1	−42.3
TS_{direct}-2 (^{4}A)	−1 536.379 982 4	98.8	−40.0
TS_{direct}-3 (^{4}A)	−1 536.382 96 92	99.5	−41.2
TS_{direct}-1a (^{6}A)	−1 536.373 917 6	98.7	−36.2
TS_{direct}-1b (^{6}A)	−1 536.374 781 6	98.5	−37.0
TS_{direct}-2 (^{6}A)	−1 536.372 602 6	98.1	−36.0
TS_{direct}-3 (^{6}A)	−1 536.376 511 2	98.2	−38.4

Table 4. Computed C−H Bond Activation Energies of 2-Methylbutane by FeO^{2+} via the Concerted Mechanism and the Radical Mechanism Measured from the Dissociation Limit

	energy (au)	ZPVE (kcal/mol)	rel energy (kcal/mol)
C_5H_{12} (^{1}A)	−197.803 231 9	100.3	
FeO^{2+} (5Σ)	−1 337.872 802 1	0.6	
TS1-1a (^{5}A)	−1 535.871 528 2	97.0	−126.5
TS1-1b (^{5}A)	−1 535.881 074 8	97.5	−132.0
TS1-2 (^{5}A)	−1 535.883 087 4	97.2	−133.6
TS1-3 (^{5}A)	−1 535.876 825 4	97.3	−129.6
TS_{direct}-1a (^{5}A)	−1 535.870 030 2	98.2	−124.5
TS_{direct}-1b (^{5}A)	−1 535.869 885 9	98.2	−124.3
TS_{direct}-2 (^{5}A)	−1 535.874 700 0	96.3	−129.2
TS_{direct}-3 (^{5}A)	−1 535.892 709 9	96.0	−140.3

Regioselectivity in 2-Methylbutane Hydroxylation. The regioselectivity in the hydroxylation reactions of 2-methylbutane by FeO^+ ($^4\Delta$ and $^6\Sigma^+$) and FeO^{2+} ($^5\Sigma^+$) is a main issue in this paper. The reactant complexes are considered from the computed energy profiles and the size of the substrate to exist as long-lived species in the sense that the binding energy is distributed among various normal modes of vibration.[22b] The large internal energy acquired is not necessarily used for C−H activation, and therefore the C−H bond is insufficiently activated to be dissociated during the formation of the reactant complexes. Considering the large C−H bond dissociation energies (∼100 kcal/mol), the C−H activation in the initial stages should play a dominant role in determining the regioselectivity in the hydroxylation reactions of 2-methylbutane. Accordingly, we compared the barrier heights of TS1's and TS_{direct}'s for the analysis of the regioselectivity. Computed energies of TS1's and TS_{direct}'s measured from the dissociation limit are listed in Tables 3 and 4, respectively.

In the abstraction reactions mediated by FeO^+ in the concerted mechanism, preference for the secondary C3−H bond is concluded, as listed in Table 3. TS1-2 lies 1.5, 4.3, and 4.5 kcal/mol below TS1-1b, TS1-1a, and TS1-3, respectively. Thus, the secondary C3−H bond is preferentially activated in the concerted mechanism. In the hydroxylation reactions mediated by FeO^{2+} in the concerted mechanism, preference for the secondary C3−H bond dissociation is also concluded; TS1-2 of the secondary C3−H bond dissociation lies 1.6, 4.0, and 7.1

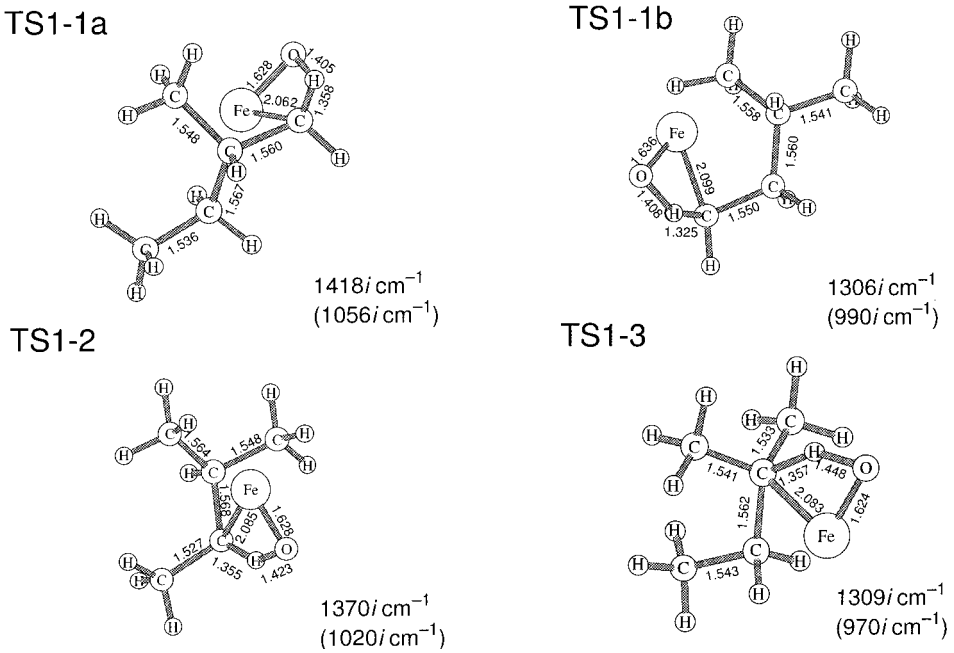

Figure 6. Ball-and-stick structures of the transition states for H atom abstractions via TS1's. Bond lengths are in Å. The values in parentheses are the imaginary frequencies in the deuterium forms.

Chart 2

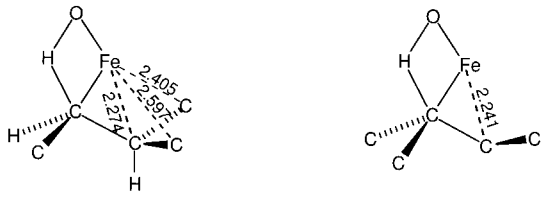

kcal/mol below TS1-1b, TS1-3, and TS1-1a, respectively, as shown in Table 4. Therefore, in the concerted mechanism these iron−oxo species prefer the secondary C3−H bond activation and exhibit the following order of regioselectivity:

2° (path 2) > 1° (path 1b) > 1° (path 1a) > 3° (path 3) for FeO^+ ($^4\Delta$)

2° (path 2) > 1° (path 1b) > 3° (path 3) > 1° (path 1a) for FeO^{2+} ($^5\Sigma^+$)

It is not intuitively clear why the secondary C−H bond dissociation is energetically more favorable than the tertiary C−H bond dissociation, but different structures of TS1's will provide a hint. Figure 6 shows computed four-centered TS1's for the concerted H atom abstractions by FeO^+. The distance between the Fe atom and the carbon atom directly activated is about 2.1 Å in both TS1-2 and TS1-3. However, the coordination environment at the iron centers is quite different in these transition states. In TS1-2 the Fe atom is close to three carbon atoms, whereas in TS1-3 the Fe atom is close to only one carbon atom, as indicated in Chart 2. The Fe···C interactions in TS1-2 should bring about substantial energetical stabilization, but in TS1-3 there are no such attractive interactions that energetically stabilize this transition state. This accounts for the preference for the secondary C−H bond dissociation in 2-methylbutane in the concerted mechanism.

How does the regioselectivity in the direct H atom abstractions via TS_{direct}'s differ from the regioselectivity in the concerted H atom abstractions via TS1's? In the direct abstraction mechanism, we expect the regioselectivity to depend on the C−H bond strength itself (see Chart 1). Computed C−H bond activation energies via TS_{direct}'s in the FeO^+ and FeO^{2+} cases are listed in Tables 3 and 4, respectively. In remarkable contrast to the concerted reactions, a strong preference for the tertiary C2−H bond is obtained in the abstraction reactions mediated by FeO^{2+} in the radical mechanism. TS_{direct}-3 of the tertiary C2−H bond dissociation by FeO^{2+} lies 11.1, 15.9, and 16.0 kcal/mol below that of the secondary C3−H bond dissociation along path 2 and those of the primary C−H bond dissociations along paths 1a and 1b, respectively. In the C−H bond dissociations via TS_{direct}, FeO^{2+} exhibits the following order of regioselectivity:

3° (path 3) > 2° (path 2) > 1° (path 1a) > 1° (path 1b) for FeO^{2+} ($^5\Sigma^+$)

This result is fully consistent with the order of the C−H bond strengths of 2-methylbutane. Hrovat and Borden demonstrated from ab initio quantum-chemical calculations that tertiary cubyl C−H bond dissociations are energetically more favorable than the methyl C−H bond dissociation in the reaction between methylcubane and an alkoxyl radical.[37] The result of the pure organic radical reactions is in good agreement with our result. Thus, if hydroxylation reactions of alkanes by enzymatic or catalytic systems occur in a radical mechanism, strong preference for tertiary C−H bond activation should occur.

Such strong preference for the tertiary C2−H bond dissociation was not seen in the FeO^+ ($^4\Delta$) case. In the

(37) Hrovat, D. A.; Borden, W. T. *J. Am. Chem. Soc.* **1994**, *116*, 6459.

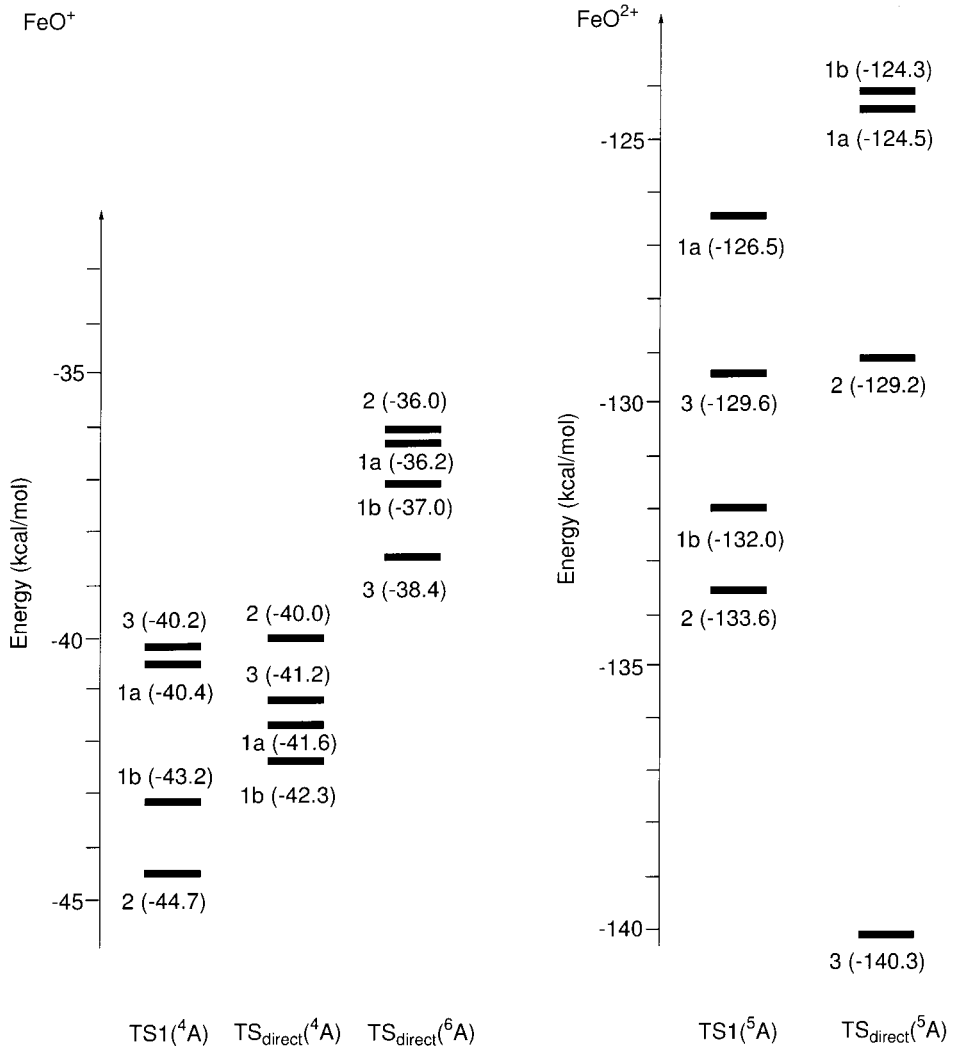

Figure 7. Computed C−H bond activation energies of 2-methylbutane by FeO^+ and FeO^{2+} via the concerted mechanism and the radical mechanism measured from the dissociation energy. Values are given in kcal/mol.

hydroxylation reactions of 2-methylbutane via TS_{direct}'s, TS_{direct}-1b lies 0.7, 1.1, and 2.3 kcal/mol below TS_{direct}-1a, TS_{direct}-3, and TS_{direct}-2, respectively. Thus, in the C−H bond dissociations via TS_{direct}s, FeO^+ exhibits the following order of regioselectivity:

$$1°\ (\text{path 1b}) > 1°\ (\text{path 1a}) > 3°\ (\text{path 3}) > 2°\ (\text{path 2})\ \text{for}\ FeO^+\ (^4\Delta)$$

We also calculated the barrier heights for the direct H atom abstractions via TS_{direct}'s by FeO^+ ($^6\Sigma^+$) in order to compare the reactivities of the quartet and the sextet species. Each potential-energy diagram in the sextet state is unstable in energy compared to that of the quartet state. TS_{direct}-3 lies 1.4, 2.2, and 2.3 kcal/mol below TS_{direct}-1b, TS_{direct}-1a, and TS_{direct}-2, respectively, as shown in Table 3. Thus, FeO^+ ($^6\Sigma^+$) exhibits the following order of regioselectivity in the C−H bond dissociations of 2-methylbutane via TS_{direct}'s. The tertiary C2−H dissociation is clearly preferred in this case.

$$3°\ (\text{path 3}) > 1°\ (\text{path 1b}) > 1°\ (\text{path 1a}) > 2°\ (\text{path 2})\ \text{for}\ FeO^+\ (^6\Sigma^+)$$

We consider that the regioselectivity in the hydroxylation reactions via TS_{direct} should be determined by the C−H bond strength of 2-methylbutane, as mentioned above. The depopulation of the C−H bonding orbitals through the interaction with FeO^{2+} is large in comparison with that of the C−H bonding orbitals through the interaction with FeO^+, as seen from computed Mulliken charges. Hence, the regioselectivity in the hydroxylation reactions via TS_{direct} by FeO^{2+} is significantly dependent on the C−H bond dissociation energies of 2-methylbutane. We schematically demonstrate in Figure 7 the computed barrier heights for the H atom abstractions by FeO^+ and FeO^{2+} via the concerted and the radical mechanisms.

Kinetic Isotope Effects (KIEs). We replaced only the H atom being abstracted with deuterium and calculated the KIEs for the C−H(D) bond dissociation mediated by FeO^+ in the concerted and the radical mechanisms. We added Wigner tunneling corrections[38] to data obtained from the transition state theory. Table 5 presents computed k_H/k_D values for the H atom abstraction via TS1's in the quartet state as a function of temperature. In the temperature range examined, there is no significant site dependence in the k_H/k_D values in the concerted H atom abstraction. Wigner

(38) Wigner, E. *Z. Phys. Chem. B* **1932**, *19*, 203. The tunneling correction coefficient is $\kappa = 1 - 1/24(h\nu^{\ddagger}/kT)^2$, where $\nu^{\ddagger}$ is the imaginary frequency relevant to a transition state.

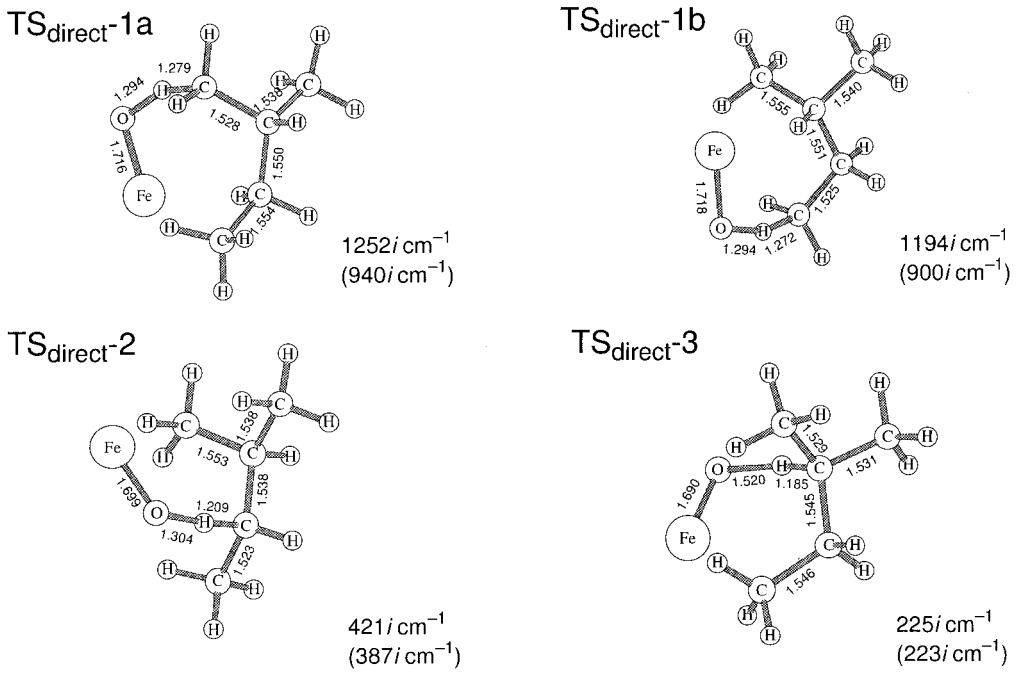

Figure 8. Ball-and-stick structures of the transition states for H atom abstractions via TS$_{direct}$'s. Bond lengths are given in Å. The values in parentheses are the imaginary frequencies in the deuterium forms.

Table 5. Computed k_H/k_D Values in H Atom Abstractions from 2-Methylbutane by FeO$^+$ via TS1 of the Quartet State, in Which Only the H Atom Being Abstracted Is Replaced with Deuterium[a]

T (K)	path 1a	path 1b	path 2	path 3
200	10.17 (15.95)	10.37 (15.58)	11.56 (18.00)	12.58 (19.52)
250	6.65 (9.89)	6.86 (9.78)	7.20 (10.61)	7.60 (11.14)
300	5.02 (7.11)	5.14 (6.98)	5.23 (7.33)	5.41 (7.52)
350	4.10 (5.55)	4.17 (5.43)	4.16 (5.58)	4.23 (5.62)
400	3.53 (4.60)	3.52 (4.42)	3.50 (4.51)	3.51 (4.48)

[a] The values in parentheses include Wigner's tunneling correction.

Table 6. Computed k_H/k_D Values in H Atom Abstractions from 2-Methylbutane by FeO$^+$ via TS$_{direct}$ of the Quartet State, in Which Only the H Atom Being Abstracted Is Replaced with Deuterium[a]

T (K)	path 1a	path 1b	path 2	path 3
200	14.13 (21.31)	13.77 (20.42)	7.10 (7.42)	4.25 (4.26)
250	8.72 (13.02)	8.53 (11.94)	4.93 (5.09)	3.23 (3.24)
300	6.34 (8.59)	6.23 (8.30)	3.88 (3.97)	2.70 (2.70)
350	5.04 (6.53)	4.97 (6.34)	3.27 (3.32)	2.38 (2.38)
400	4.23 (5.28)	4.19 (5.15)	2.88 (2.92)	2.16 (2.16)

[a] The values in parentheses include Wigner's tunneling correction.

tunneling corrections enhanced the isotope effects, as expected; the computed k_H/k_D values are about 1.5 times larger when we take the tunneling effect into account. Table 6 presents computed k_H/k_D values for the direct H atom abstraction via TS$_{direct}$'s in the quartet state. In the radical mechanism, there appears significant site dependence in the k_H/k_D values. For example, at 300 K the computed k_H/k_D values for the primary C1−H and C4−H, secondary C3−H, and tertiary C2−H bond dissociations are 6.34 (8.59), 6.23 (8.30), 3.88 (3.97), and 2.70 (2.70), respectively, from the transition state theory (with Wigner tunneling corrections). This result shows that the k_H/k_D values with respect to TS$_{direct}$'s decline in the order 1° > 2° > 3°, in remarkable contrast to the general trend of the concerted mechanism mentioned above. No explicit tunneling effect is observed in the secondary C3−H and tertiary C2−H bond dissociations, due to the fact that there is little isotope effect in the imaginary frequencies relevant to the corresponding TS$_{direct}$'s (see Figures 6 and 8). We can therefore determine how alkanes are hydroxylated by an iron−oxo species in the gas phase and catalytic systems in view of the measured and computed k_H/k_D values.

Here we consider why the k_H/k_D values depend on the positions of 2-methylbutane in the direct H atom abstraction via TS$_{direct}$. The k_H/k_D values depend on the difference in the zero-point vibrational energies of the C−H and C−D stretching vibrations in general, and we may obtain useful information from the structures of TS1's and TS$_{direct}$'s shown in Figures 6 and 8, respectively. The four-centered structures of TS1's are similar because the existence of the Fe−C bonds can fix the four-centered structures. For example, the C−H bonds being dissociated in TS1's were calculated to be about 1.35 Å in all the cases; as a consequence, the vibrational structures of TS1's are similar. This is the reason that the k_H/k_D values do not depend on the positions of 2-methylbutane in the concerted mechanism. On the other hand, the nearly linear structures (C−H−O) in TS$_{direct}$'s are slightly different in shape, due to the lack of the Fe−C bonds; the distances of the C−H bonds being dissociated and the O−H bonds being formed in TS$_{direct}$'s change significantly. For example, the C−H bond distances in TS$_{direct}$'s were calculated to be about 1.27 Å on the primary C1 and C4 carbon atoms, 1.209 Å on the secondary C3 carbon atom, and 1.185 Å on the tertiary C2 carbon atom. The geometrical variations in TS$_{direct}$'s can lead to different vibrational structures. The differences in the geometries and the vibrational structures will lead to different k_H/k_D values in the radical mechanism via TS$_{direct}$.

Conclusion

We studied the regioselectivity in 2-methylbutane hydroxylations mediated by FeO^+ and FeO^{2+} via TS1, the transition state of concerted H atom abstraction, and TS_{direct}, the transition state of direct H atom abstraction. We analyzed from DFT calculations the reaction pathways and the energetics for four kinds of hydroxylation reactions of 2-methylbutane that lead to primary (1°), secondary (2°), and tertiary (3°) alcohols. The concerted mechanism via the four-centered transition state (TS1) is energetically more favorable than the radical mechanism via the transition state with a nearly linear C−H−O array (TS_{direct}) in most cases, except for a case generating a tertiary carbon radical intermediate. The regioselectivity in the hydroxylation reactions by FeO^+ and FeO^{2+} in the concerted mechanism declines in the order 2° > 1° > 3°. In contrast to the concerted mechanism, the regioselectivity in the hydroxylation reactions mediated by FeO^{2+} in the radical mechanism declines in the order 3° > 2° > 1°. Moreover, we calculated and analyzed the KIEs in both mechanisms on the basis of the transition state theory. Computed k_H/k_D values in the concerted mechanism do not show significant site dependence. On the other hand, the order of k_H/k_D values in the radical mechanism is 1° > 2° > 3° and there is significant site dependence in the k_H/k_D values.

Acknowledgment. Thanks are due to Yoshihito Shiota for computational assistance. K.Y. acknowledges a Grant-in-Aid for Scientific Research on the Priority Area "Molecular Physical Chemistry" from the Ministry of Education, Science, Sports and Culture of Japan and the Iwatani Naoji Foundation's Research Grant for their support of this work. Computations were partly carried out at the Supercomputer Laboratory of Kyoto University and at the Computer Center of the Institute for Molecular Science.

OM000811B